Spontaneous generation of local *CP* violation and inverse magnetic catalysis

Lang Yu,[1,*] Hao Liu,[1,†] and Mei Huang[1,2,‡]

[1]*Institute of High Energy Physics, Chinese Academy of Sciences, Beijing 100049, China*
[2]*Theoretical Physics Center for Science Facilities, Chinese Academy of Sciences, Beijing 100049, China*

(Received 8 June 2014; revised manuscript received 23 June 2014; published 6 October 2014)

In the chiral symmetric phase, the polarized instanton–anti-instanton molecule pairing induces a nontrivial repulsive interaction in the isoscalar axial-vector channel. As a consequence, one unusual property is observed that in the chiral restoration phase, there is a first order phase transition for the spontaneous generation of local charge parity ($\mathcal{CP}$) violation and chirality imbalance. Furthermore, it is found that external magnetic fields will lower the critical temperature for the local $\mathcal{CP}$-odd phase transition and catalyze the chirality imbalance, which destroys the chiral condensate with pairing quarks between different chiralities. A reasonable strength of the repulsive interaction in the isoscalar axial-vector channel can naturally explain the inverse magnetic catalysis around the critical temperature under external magnetic fields.

DOI: 10.1103/PhysRevD.90.074009 PACS numbers: 12.38.Aw, 12.38.Mh

I. INTRODUCTION

Quantum chromodynamics (QCD) is widely accepted to be the fundamental theory of the strong interactions. The study of the QCD phase structure and phase diagram has always been one of the most attractive topics to understand the nature of the strong interactions. In particular, the nonperturbative features of QCD can be affected significantly by thermal excitations at high temperatures and by strong external magnetic fields. This kind of investigation has realistic relevance to phenomenology in noncentral heavy ion collisions, in which hot quark-gluon plasma with a strong magnetic field is generated. The strength of the magnetic fields can reach up to $\sqrt{eB} \sim 0.1$ GeV at Relativistic Heavy Ion Collider (RHIC) and $\sqrt{eB} \sim 0.5$ GeV at the Large Hadron Collider (LHC) [1–4]. Hence, heavy ion collisions provide a most intriguing platform for us to probe the effects of high temperatures and strong magnetic fields on the properties of QCD.

One of the most important aspects of the QCD at zero and finite temperatures is the spontaneous breaking of chiral symmetry. The chiral condensate is an order parameter in the chiral limit by assuming zero current quark masses, which offers a nonzero vacuum expectation value in the hadronic phases and vanishes above the chiral transition temperature T_c where chiral symmetry is restored. In nature, although the chiral condensate is only an approximate order parameter as a results of the nonzero but small quark masses, it still characteristically describes the chiral phase transition between the hadronic and the quark-gluon plasma phase. Therefore, the behavior of the chiral condensate can help us investigate the QCD phase diagram and the properties of the strong interactions.

When considering the impact of magnetic fields on the chiral condensate of QCD at zero chemical potential, an interesting consequence has been recognized since the 1990s, which is the so-called magnetic catalysis [5–8]. It refers to an effect that the chiral condensate increases with the increasing B and thus the transition temperature T_c grows with B as well. This has been verified by almost all earlier low-energy effective models and approximations to QCD [5–7,9–20] as well as lattice simulations [21–25] in the past twenty years, although several model calculations, such as the two-flavor chiral perturbation theory [26], the linear sigma model without vacuum corrections [27], and the bag model [28], exceptionally obtained a decreasing $T_c(B)$ function. However, a recent lattice result [29] surprisingly shows that the transition temperature T_c significantly decreases with the increasing magnetic field. In addition, the dependence of the chiral condensate on the external magnetic field varies for different temperature regions [30]. At zero and low temperatures, the increasing behavior of the chiral condensate with B is confirmed, which corresponds to the effect of magnetic catalysis. And then at crossover region, where the temperature is close to but below $T_c(eB = 0)$, the chiral condensate increases first as B grows and then begins to decrease at a certain magnetic field value, showing a humplike structure. When above $T_c(eB = 0)$, the chiral condensate shows a monotonously decreasing dependence on B. This phenomenon is in conflict with previous calculations, and the partly decreasing behavior of the chiral condensate with the increasing B around T_c is called inverse magnetic catalysis.

The phenomenon of inverse magnetic catalysis around T_c calls for new understandings in theory, although the decreasing dependence of T_c on B is expected to be a very

*yulang@mail.ihep.ac.cn
†haoliu@mail.ihep.ac.cn
‡huangm@mail.ihep.ac.cn

small effect in the quark-gluon plasma produced by noncentral heavy ion collisions at RHIC and LHC, where the magnetic field decreases extremely fast. There have been several proposals [31–35] trying to understand the underlying mechanism of this puzzle related to the chiral phase transition, which is quite different from our conventional understanding and predictions. One of the most competitive mechanisms to explain inverse magnetic catalysis near T_c is suggested to be attributed to the local chirality imbalance induced by the nontrivial topological gluon configuration. The action of a certain gluon configuration is determined by the topological charge

$$Q_T = \frac{1}{32\pi^2}\int d^4x F^{a\mu\nu}\tilde{F}^a_{\mu\nu}, \tag{1}$$

where $F^{a\mu\nu}$ and $\tilde{F}^a_{\mu\nu} = \frac{1}{2}\epsilon_{\mu\nu\rho\sigma}F^{a\rho\sigma}$ denote the gauge field strength tensor and its dual, respectively. Furthermore, since $Q_T = \Delta N_{CS} = N_{CS}(t=+\infty) - N_{CS}(t=-\infty)$, the gauge field configuration with $Q_T \neq 0$ connects different topological vacua characterized by different Chern-Simons numbers. The chirality imbalance is induced by the nonzero topological charge through the axial anomaly of QCD,

$$\Delta N_5 = \int d^4x \partial_\mu j^\mu_5 = -2N_f Q_T, \tag{2}$$

where N_f is the number of flavors, $\Delta N_5 = N_5(t=+\infty) - N_5(t=-\infty)$, with $N_5 = N_R - N_L$ denoting the number difference between right- and left-hand quarks, and $\partial_\mu j^\mu_5 = -\frac{N_f}{16\pi^2}F^{a\mu\nu}\tilde{F}^a_{\mu\nu}$ in the chiral limit, associated with the isospin singlet axial-vector current $j^\mu_5 = \bar{\psi}\gamma^\mu\gamma^5\psi$. Hence, the configurations with nonzero topological charge, depending on the sign of the Q_T, can transform left- into right-hand quarks or vice versa, and lead to the breaking of the parity ($\mathcal{P}$) and charge parity ($\mathcal{CP}$) symmetry. At zero and low temperatures, the instantons in a random liquid state are the configurations with finite topological charge (instantons with $Q_T = 1$, while anti-instanton with $Q_T = -1$) responsible for the tunneling transitions and are expected to be thermally suppressed at high temperature. The configurations responsible for thermal topological transitions, which occur at a copious rate at high temperatures compared to the instantons, are called sphalerons. Because of the existence of QCD sphalerons, chirality can be produced in the high temperature phase of QCD. Moreover, in fact, there is no direct $\mathcal{P}$ and $\mathcal{CP}$ violation in QCD, so the chirality vanishes on average and can only occur locally in the QCD vacuum. It means that the probability to generate either a sphaleron (instanton) or an antisphaleron (anti-instanton) is equal. In this scenario, there will be some domains with net topological charge Q_T, while some other domains with net topological charge $-Q_T$. Thus, net chirality imbalance is induced in these two kinds of domains separately but the average chirality is zero for the whole QCD vacuum system. Furthermore, it has been proposed that an interplay between a nonzero local chirality and a magnetic field induces a current along the magnetic field, which is the so-called chiral magnetic effect (CME) [36–38]. It will lead to a charge separation effect that may be observed experimentally in the noncentral heavy ion collisions. The recent observation of charge azimuthal correlations at RHIC and LHC [39–41] possibly resulted from the CME with local $\mathcal{P}$ and $\mathcal{CP}$ violation.

However, it is difficult to describe the sphaleron transition process in a dynamical way. In this work we present a dynamical mechanism based on the instanton–anti-instanton ($I\bar{I}$) molecule picture [42–45], which is valid at finite temperature $T \gtrsim T_c$. It has been suggested that although individual instantons and anti-instantons are strongly suppressed in the chirally restored phase, they still keep sizable density near and above T_c and are paired up into the ordered $I\bar{I}$ molecules when approaching to T_c from below. Therefore, the interacting instanton–anti-instanton molecules can be regarded as one of the possible mechanisms responsible for a variety of nonperturbative effects of QCD in the region $T \simeq T_c - 2T_c$ [44,45]. In this scenario, the corresponding effective Lagrangian density is derived and expressed in the form of the four-fermion interactions similar to the Nambu-Jona-Lasinio (NJL) model [44]. Particularly, an unconventional prediction was proposed that the isoscalar axial-vector interaction is repulsive. This four-quark interaction channel will naturally induce local chirality imbalance and dynamical chiral chemical potential in QCD at high temperatures near T_c. And also it is found that the increasing magnetic fields help to lower the critical temperature for the appearance of the local chirality. Hence, the pairing of the chiral condensate is affected by the chirality imbalance and the chiral phase transition is modified by the external magnetic fields at the temperatures around T_c correspondingly. Moreover, the average net topological charge is zero in the $I\bar{I}$ molecule picture because of the equal number between instantons and anti-instantons. One domain with a number of instantons contains more left-hand quarks, while the other domain with the same number of anti-instantons contains more right-hand quarks. This is in agreement with our assumption with respect to the local chirality imbalance.

The paper is organized as follows. In Sec. II, we give a general description of the NJL model with consideration of the effective four-quark interaction in the axial-vector channel adopted in this paper, and discuss the unusual prediction upon this channel stemming from the interacting $I\bar{I}$ molecule model (IIMM) intensively. In Sec. III, we derive the thermodynamical potential by using the corresponding Lagrangian density in the mean field approximation. In Sec. IV, we present the results of the numerical calculations and related discussion. Finally, we give conclusions and discussions in Sec. V.

II. MODEL WITH THE AXIAL-VECTOR INTERACTION

We investigate the chiral phase transition of QCD at zero and finite temperatures in the presence of magnetic fields in the framework of the NJL model [46–51]. The Lagrangian density of our model is given by

$$\mathcal{L} = \bar{\psi} i\gamma_\mu D^\mu \psi + G_S[(\bar{\psi}\psi)^2 + (\bar{\psi} i\gamma^5 \boldsymbol{\tau}\psi)^2] - G_V(\bar{\psi}\gamma^\mu\psi)^2 - G_A(\bar{\psi}\gamma^\mu\gamma^5\psi)^2. \tag{3}$$

In the above equation, ψ corresponds to the quark field of two light flavors u and d. G_S, G_V, and G_A are the coupling constants with respect to the scalar (pseudoscalar), the vector isoscalar, and the axial-vector isoscalar channels, respectively. The covariant derivative, $D_\mu = \partial_\mu - iq_f A_\mu$, couples quarks to an external magnetic field $\boldsymbol{B} = (0, 0, B)$ along the positive z direction, via a background field, for example, $A_\mu = (0, 0, -Bx, 0)$. And q_f is defined as the electric charge of the quark field. Here, we will just work in the chiral limit, since the current masses of two light quark flavors are only a few MeV and their influence in the physical world can be negligible as compared to the temperature. In particular, although it has been shown in Ref. [52] that the chiral limit is trivial and the quark masses play an important role in magnetic perturbative QCD, the effects of the current masses of light quarks on the chiral phase transition are very small in our scenario in which the temperature is not large enough to make the perturbation theory reliable, and the dynamic quark masses stemming from the chiral condensate is much more important. Furthermore, one can find that the vector isoscalar and axial-vector isoscalar channels add to the simplest traditional $SU(2)_f$ NJL model. It will be shown in the following that the axial-vector isospin-scalar channel becomes important for the physics related to chiral phase transition at large temperature $T \simeq T_c$.

In fact, this type of Lagrangian density (3) has been studied by a generalized $SU(2)_f$ NJL model with effective four-fermion interactions in Ref. [48,49], which is Fierz invariant and respects $SU(2)_V \otimes SU(2)_A \otimes U(1)_V \otimes U(1)_A$ symmetry. Its most general form of the effective four-quark interactions for two light flavors is given by

$$\begin{aligned}\mathcal{L}^{(4)}_{\text{general}} = \frac{1}{2}G_1[(\bar{\psi}\tau^a\psi)^2 + (\bar{\psi}\tau^a i\gamma^5\psi)^2] \\ -\frac{1}{2}G_2[(\bar{\psi}\tau^a\gamma^\mu\psi)^2 + (\bar{\psi}\tau^a\gamma^\mu\gamma^5\psi)^2] \\ -\frac{1}{2}G_3[(\bar{\psi}\tau^0\gamma^\mu\psi)^2 + (\bar{\psi}\tau^0\gamma^\mu\gamma^5\psi)^2] \\ -\frac{1}{2}G_4[(\bar{\psi}\tau^0\gamma^\mu\psi)^2 - (\bar{\psi}\tau^0\gamma^\mu\gamma^5\psi)^2] \\ + \mathcal{L}^{(4)}_{\text{color octet}},\end{aligned} \tag{4}$$

where $\mathcal{L}^{(4)}_{\text{color octet}}$ is the color-octet part of $\mathcal{L}^{(4)}_{\text{general}}$ (not shown explicitly here). G_i are four independent coupling constants and τ^a is a four-vector with components $(1, \vec{\boldsymbol{\tau}})$, which are unit and Pauli matrices in isospin space, respectively. Comparing Eq. (3) with Eq. (4), one can find the relations between the coupling constants:

$$G_S = \frac{1}{2}G_1, \qquad G_V = \frac{1}{2}(G_2 + G_3 + G_4), \qquad G_A = \frac{1}{2}(G_2 + G_3 - G_4). \tag{5}$$

Conventionally, the value of G_S is determined by fitting the experimental data with a globe cutoff in the numerical calculations, while the values of G_V and G_A are fixed by obtaining the ratios of G_V/G_S, G_A/G_S, or G_A/G_V in other models or some other related experimental data fitting. The signs and magnitudes of G_S, G_V, and G_A determine the properties and strength of the corresponding four-quark interactions.

In the simplest NJL model with only scalar isoscalar and pseudoscalar isoscalar channels, which can produce the low-energy phenomena related to chiral symmetry breaking at $T = 0$, has a positive G_S. This is consistent with the effective four-quark interactions induced by the random instanton liquid model (RILM) [53–55], which is described by the famous 't Hooft effective interaction [56]. The RILM also gives a very successful phenomenology of the QCD vacuum at $T = 0$, since instantons provide a mechanism for chiral symmetry breaking and generate strong interactions between light quarks. One can find that it leads to attractive interactions in the π and σ channels, and no interactions in the vector and axial-vector channels, to the first order in the instanton density. Therefore, we obtain in RILM that G_S is positive, which can be determined by the instanton density, and $G_V = G_A = 0$.

Furthermore, as we know, the fundamental quark currents in QCD are color currents $J^a_\mu = \bar{\psi}\gamma^\mu t^a\psi$, which arise from the one gluon exchange approximation [49]. As a consequence, a simple example of a local four-quark interaction described by two such currents is given by

$$\mathcal{L}^{(4)}_c = -G_c(\bar{\psi}\gamma^\mu t^a\psi)^2, \tag{6}$$

where G_c is a coupling constant and t^a are $SU(3)_{\text{color}}$ generators. By taking Fierz transformation, one can get

$$G_S = 2G_V = 2G_A. \tag{7}$$

Similarly, based on a colored current-current but nonlocal interaction, the global color model of QCD was proposed and successfully explained many properties of nonperturbative QCD with relatively strong couplings [57–60]. Thus, it suggests that G_S, G_V, and G_A are positive at zero and low temperatures.

A full consideration of the NJL model with a generalized Lagrangian density (4) in Ref. [49] gives predictions that $G_S/G_V \simeq 1.5$ and $G_A/G_V \simeq 2.5$ by fitting the mesonic properties. It means that G_S, G_V, and G_A are all nonzero and positive. Especially, the positive sign of G_A is ensured by the fact that the value of the flavor singlet axial constant g_A^0 deduced from the EMC data [61] is smaller than 1 [48,49]. Since the calculations in the context of all models above give successful description of the low-lying hadrons and QCD vacuum at zero and finite but low temperature, it is reasonable to believe that, at zero and low temperature, G_S, G_V, and G_A should be positive.

At zero and low temperature, since the 't Hooft interaction is dominant, the random instantons play an important role in chiral symmetry breaking. However, at high temperature near the chiral phase transition, the instantons are no longer random, but become correlated. Therefore, it was suggested that the growing correlations between instantons and anti-instantons near T_c lead to the decrease of random instantons and the increase of instanton–anti-instanton molecule pairs [42–44]. It means that the random instantons and anti-instantons are not annihilated but paired up into the correlated $I\bar{I}$ molecules when chiral phase transition happens. Thus, for $T \gtrsim T_c$, the resulting Fierz symmetric Lagrangian density with the effective local four-quark interactions induced by $I\bar{I}$ molecules [44] reads

$$\mathcal{L}_{\text{mol sym}} = G\left\{\frac{2}{N_c^2}[(\bar{\psi}\tau^a\psi)^2 - (\bar{\psi}\tau^a\gamma^5\psi)^2] - \frac{1}{2N_c^2}[(\bar{\psi}\tau^a\gamma^\mu\psi)^2 + (\bar{\psi}\tau^a\gamma^\mu\gamma^5\psi)^2] + \frac{2}{N_c^2}(\bar{\psi}\gamma^\mu\gamma^5\psi)^2\right\} + \mathcal{L}_8, \tag{8}$$

where $\mathcal{L}_8$ denotes the color-octet part of the interactions. G is the coupling constant, which is determined by the number density of $I\bar{I}$ molecule pairs. Compared with Eq. (3), the molecule-induced effective Lagrangian gives

$$G_S = \frac{2G}{N_c^2}, \qquad G_V = \frac{G}{2N_c^2}, \qquad G_A = -\frac{3G}{2N_c^2}. \tag{9}$$

It indicates that (1) the π, σ, δ, η', ω, ρ, and a_1 channels are attractive as a result of positive G_S and G_V, which are the same as the generalized NJL model in Refs. [48,49] and (2) the axial-vector isoscalar channel f_1 is repulsive because of negative G_A, which is quite different from all the above models. Therefore, when approaching to T_c from below, it seems that the coupling constant G_A flips the sign from positive to negative, based on the $I\bar{I}$ molecule model. And G_A should be negative near and above the critical temperature of chiral phase transition. The unconventional repulsive axial-vector interaction leads to a repulsive axial-vector mean field in the spacelike components but an attractive one in the timelike components, by following the discussion in Ref. [62]. This effect turns out to be very important in explaining inverse magnetic catalysis in our model, which will be discussed in Sec. IV. In addition, the molecule-induced effective Lagrangian (8) is derived by averaging over possible molecule orientation, with the relative color orientation fixed. Thus one gets $G_V = \frac{1}{4}G_S$ and $G_A = -\frac{3}{4}G_S$ by Eq. (9). If the molecules are completely polarized near T_c, molecules are polarized in the time direction and therefore we get an effective Lagrangian similar to Eq. (8) but with all vector (or axial-vector) interactions modified according to $\bar{\psi}\gamma^\mu\Gamma\psi \to 4\bar{\psi}\gamma^0\Gamma\psi$ [44,63]. In this situation, one can find that $G_V = G_S$ and $G_A = -3G_S$. It means that the magnitudes of G_V and G_A will increase due to the polarization of the molecules. Therefore, even when $T \gtrsim T_c$, G_A is still temperature dependent and related to the polarization strength for the molecules.

Finally, we make some general remarks about the coupling constants G_S, G_V, and G_A. First, G_S and G_V are always positive no matter what temperature it is. Second, G_A is positive at zero and low temperature and is negative at the temperature above T_c. Third, G_S, G_V, and G_A are actually all T dependent. However, G_V is not needed to be considered since it is not related to inverse magnetic catalysis. For simplicity, G_S and G_A in our calculations are both treated as constants for the whole temperature region and not affected by the external magnetic field as well. G_S is fitted as a positive parameter without considering the temperature dependence. As for G_A, we will treat it as a free parameter. It is found in our calculations that, no matter what values we use, the behavior of quark condensates below T_c obtains little influence. It means that it does not make any difference even if we use a negative value for the whole temperature range. In addition, the inverse magnetic catalysis effects become evident only when near critical temperature. This is consistent with the valid region of the $I\bar{I}$ molecule model with a negative G_A. As a consequence, our results about the chiral phase transition should also be always convincing although a negative constant is used for G_A in the whole T range.

III. MEAN FIELD APPROACH

At mean field level, the corresponding Lagrangian from Eq. (3) can be given by the following formula:

$$\mathcal{L} = -\frac{\sigma^2}{4G_S} + \frac{\tilde{\mu}_5^2}{4G_A} + \bar{\psi}(i\gamma_\mu D^\mu - \sigma + \tilde{\mu}_5\gamma^0\gamma^5)\psi, \tag{10}$$

with $\sigma = -2G_S\langle\bar{\psi}\psi\rangle$ and $\tilde{\mu}_5 = -2G_A\langle\bar{\psi}\gamma^0\gamma^5\psi\rangle$. Here, we just keep the scalar isoscalar and the axial-vector isoscalar channels, since only these two channels are particularly significant to the chiral phase transition. The scalar density $\langle\bar{\psi}\psi\rangle$ is the order parameter for chiral phase transition, and the chirality density $\langle j_5^0\rangle = \langle\bar{\psi}\gamma^0\gamma^5\psi\rangle$ is the zeroth component of expectation value for the axial current $j_5^\mu = \bar{\psi}\gamma^\mu\gamma^5\psi$, and it describes the chirality imbalance. $\langle\bar{\psi}\gamma^0\gamma^5\psi\rangle$ should be zero on average because of the equal numbers for the right-hand and left-hand quarks, no matter what the temperatures are. The vanishing average value of $\langle\bar{\psi}\gamma^0\gamma^5\psi\rangle$ can be understood as the formation of local domains, each one having a nonzero $\langle\bar{\psi}\gamma^0\gamma^5\psi\rangle$ value. And the probability to create a domain with a positive $\langle\bar{\psi}\gamma^0\gamma^5\psi\rangle$ is the same as the probability to create a domain with a negative $\langle\bar{\psi}\gamma^0\gamma^5\psi\rangle$. Here, we focus on studying the domains with a positive $\langle\bar{\psi}\gamma^0\gamma^5\psi\rangle$ in equilibrium states. The nonzero value of $\langle\bar{\psi}\gamma^0\gamma^5\psi\rangle$ for the local domains should be induced by the interactions of the system itself and can be determined by its own equilibrium conditions.

Comparing σ with $\tilde{\mu}_5$, one can find some similarities between them. The four-quark interaction in the scalar isoscalar channel leads to a dynamic quark mass σ arising from the scalar density $\langle\bar{\psi}\psi\rangle$, while the interaction in the axial-vector isoscalar channel leads to a dynamic axial chemical potential $\tilde{\mu}_5$ arising from the chiral density $\langle\bar{\psi}\gamma^0\gamma^5\psi\rangle$. Since $\tilde{\mu}_5$ is an induced quantity generated dynamically by the axial-vector interaction and directly related to the nonzero $\langle\bar{\psi}\gamma^0\gamma^5\psi\rangle$ in the local domains, it is not associated with a conserved charge. Therefore, we treat it more like a kind of dynamical condensate in analogy with σ and do not need to introduce an artificial chiral chemical potential. Moreover, the minimization of the thermodynamical potential with respect to σ and $\tilde{\mu}_5$ will determine the dependence of them on magnetic fields and temperatures.

Thus, we begin to find the thermodynamical potential in the following. By integrating out the quark fields ψ, one gets the thermodynamical potential per unit volume Ω in the mean field approximation,

$$\begin{aligned}\Omega = &\frac{\sigma^2}{4G_S} - \frac{\tilde{\mu}_5^2}{4G_A}\\ &- N_c\sum_{f=u,d}\frac{|q_fB|}{2\pi}\sum_{s,k}\alpha_{sk}\int_{-\infty}^{\infty}\frac{dp_z}{2\pi}f_\Lambda^2(p)\omega_{sk}(p)\\ &- 2N_cT\sum_{f=u,d}\frac{|q_fB|}{2\pi}\sum_{s,k}\alpha_{sk}\int_{-\infty}^{\infty}\frac{dp_z}{2\pi}\\ &\times\ln(1+e^{-\omega_{sk}/T}),\end{aligned} \tag{11}$$

where

$$\omega_{sk} = \sqrt{\sigma^2 + [|\boldsymbol{p}| + s\tilde{\mu}_5\mathrm{sgn}(p_z)]^2} \tag{12}$$

are the eigenvalues of the Dirac operator with spin factors $s = \pm 1$,

$$\boldsymbol{p}^2 = p_z^2 + 2|q_fB|k, \tag{13}$$

and $k = 0, 1, 2, \ldots$ is a non-negative integer number labeling the Landau levels. The spin degeneracy factor is

$$\alpha_{sk} = \begin{cases}\delta_{s,+1} & \text{for } k = 0, qB > 0,\\ \delta_{s,-1} & \text{for } k = 0, qB < 0,\\ 1 & \text{for } k \neq 0.\end{cases} \tag{14}$$

Following Ref. [38] we use a smooth regularization form factor

$$f_\Lambda(p) = \sqrt{\frac{\Lambda^{2N}}{\Lambda^{2N} + |\boldsymbol{p}|^{2N}}}, \tag{15}$$

where we take $N = 5$. Now, by making use of Eq. (11), σ and $\tilde{\mu}_5$ can be determined self-consistently by solving the saddle point equations

$$\frac{\partial\Omega}{\partial\sigma} = \frac{\partial\Omega}{\partial\tilde{\mu}_5} = 0. \tag{16}$$

IV. NUMERICAL RESULTS AND DISCUSSION

In this section, we provide the numerical calculation results of σ and $\tilde{\mu}_5$ at zero and finite temperature in a uniform magnetic field by using Eq. (16) and analyze their effects on the chiral phase transition and inverse magnetic catalysis. Our model parameters are fitted by reproducing the pion decay constant and the quark condensate in the vacuum. They are given by $\Lambda = 626.76$ MeV and $G_S\Lambda^2 = 2.02$. These parameters correspond to $f_\pi = 92.3$ MeV, the vacuum quark condensate $\langle\bar{u}u\rangle = -(251)^3$ MeV, and the constituent quark mass $M = 325$ MeV. As we only have a free parameter G_A, a ratio $r_A = G_A/G_S$ is defined to describe the variation of G_A.

Figure 1 shows the quark condensate σ and dynamical chiral chemical potential $\tilde{\mu}_5$ as a function of T at $r_A \geq 0$, and $r_A = -0.50, -0.75, -0.85$, and -1.0 in the case of $eB = 0$. For $r_A = 0$ and $r_A > 0$, the effective potential Ω has no minimum with respect to $\tilde{\mu}_5$ at finite temperature and there is no chirality imbalance induced in the chiral symmetric phase. Therefore, one can only observe the chiral phase transition at T_c, which is of second order in the chiral limit.

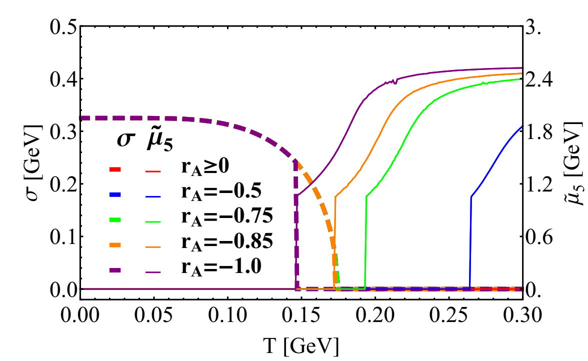

FIG. 1 (color online). Quark condensate σ and dynamical chiral chemical potential $\tilde{\mu}_5$ as a function of T at $eB = 0$ for several values of r_A.

However, when r_A is negative, a different situation occurs that the potential Ω has two local minima. One is the original trivial minimum with nonzero chiral condensate; the other one has a zero quark condensate σ but nonzero dynamical chiral chemical potential $\tilde{\mu}_5$ due to the attractive mean field in the timelike component of the axial-vector interaction. When the temperature is low, the former one is lower than the latter one, so it is a global minimum and corresponds to a stable QCD vacuum; whereas, when the temperature reaches T_{5c}, a critical temperature for nonzero $\tilde{\mu}_5$, the latter minimum turns to be lower and becomes the new stable QCD vacuum state, even if the magnetic field is zero. Therefore, the competition between the quark condensate σ and the dynamical chiral chemical potential $\tilde{\mu}_5$ results in the chirality imbalance at high temperatures above T_{5c}. Therefore, a dynamical chiral chemical potential $\tilde{\mu}_5$ is spontaneously generated by repulsive quark interaction in the isoscalar axial-vector channel. It means that local $\mathcal{P}$-odd and $\mathcal{CP}$-odd domains should exist in the quark-gluon plasma produced in heavy ion collisions, and thus the chiral magnetic effect is expected to take place when the external magnetic filed is present. It is noticed that the local $\mathcal{CP}$-odd phase transition for $\tilde{\mu}_5$ is always of first order. The increase of the magnitude $|r_A|$ will lower the critical temperature T_{5c}. When $r_A > -0.85$, it is found that the chiral phase transition and the local $\mathcal{CP}$-odd phase transition are independent with $T_{5c} > T_c$; one is of second order and the other one is of first order. When $r_A \leq -0.85$, the chiral phase transition and the local $\mathcal{CP}$-odd phase transition are locked with $T_{5c} = T_c$, and both are of first order.

When the external magnetic field turns on, we can investigate the effect of magnetic field on the chiral phase transition and the local $\mathcal{CP}$-odd phase transition in Fig. 2 for $r_A = -0.50, -0.75, -0.85$, and -1.0. For the cases of $r_A = -0.50$ and -0.75, when the magnetic field is not strong enough, the second order chiral phase transition and the first order local $\mathcal{CP}$-odd phase transition are separated with $T_{5c} > T_c$, so that T_c increase with eB and T_{5c} decreases with eB; when the magnetic field is strong enough, the chiral phase transition and local $\mathcal{CP}$-odd phase transition happen together at $T_c = T_{5c}$, and both are of first order. For the cases of $r_A = -0.85$ and -1.0, two kinds of phase transitions always occur at the same temperatures and both are of first order. With the increase of the magnetic field, it is found that, at low temperature, the magnitude of chiral condensate σ increases with magnetic field, which is the familiar magnetic catalysis. However, the critical temperature for local chirality imbalance T_{5c} is lowered by the magnetic field, which means that the magnetic field is the catalyzer of the local chirality imbalance. Hence, the increasing of the magnetic field decreases the critical temperature T_c and the inverse magnetic catalysis effect becomes understandable for the whole magnetic fields

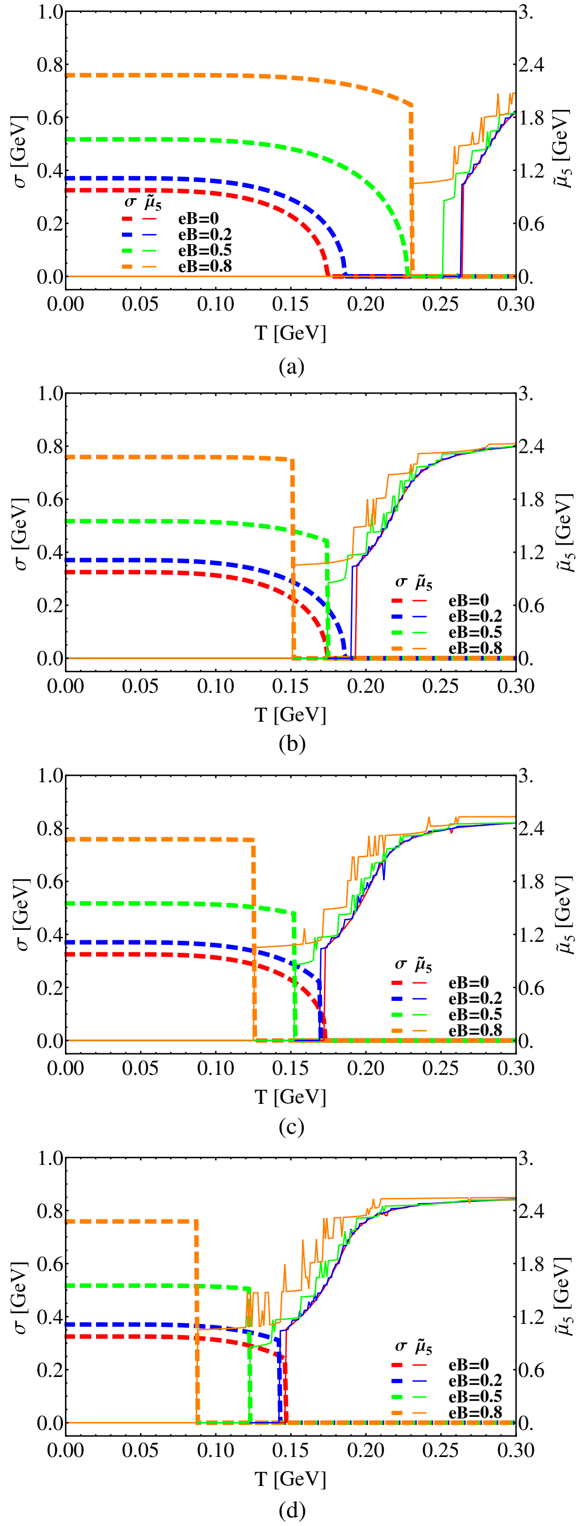

FIG. 2 (color online). Quark condensate σ and dynamical chiral chemical potential $\tilde{\mu}_5$ as a function of T at $r_A = -0.50$, -0.75, -0.85, and -1.0 for different values of eB. (a) σ and $\tilde{\mu}_5$ at $r_A = -0.50$ for different values of eB. (b) σ and $\tilde{\mu}_5$ at $r_A = -0.75$ for different values of eB. (c) σ and $\tilde{\mu}_5$ at $r_A = -0.85$ for different values of eB. (d) σ and $\tilde{\mu}_5$ at $r_A = -1.0$ for different values of eB.

region. In addition, one can observe that the curves of $\tilde{\mu}_5$ in Fig. 2 become less smooth when eB increases. This is because the increase of the strength of the magnetic field gives rise to a decrease of the number of the filled Landau levels in the numerical calculations, and the oscillations in the graphs become more intense correspondingly.

In Fig. 3, we show the critical temperature T_c and T_{5c} for chiral phase transition as a function of eB with different values of $r_A = 0$, -0.50, -0.75, -0.85, and -1.0. It is clearly shown that when $r_A = 0$, i.e., no repulsive iso-scalar axial-vector interaction, the critical temperature increases with magnetic field, and shows magnetic catalysis effect. When the magnitude of $|r_A|$ increases and $r_A > -0.85$, the critical temperature T_c shows a nonmonotonic behavior, first increasing with eB then decreasing with eB. When $r_A \le -0.85$, the critical temperature T_c decreases monotonically with eB. However, the value of T_c at $eB = 0$ for $r_A < -0.85$ is lower than that of at $r_A = 0$. With the magnitude of $r_A = -0.85$, the monotonic decreasing T_c from $T_c = T_c(r_A = 0)$ with eB is in agreement with the inverse magnetic catalysis observed in lattice [29]. As for T_{5c}, it always decreases monotonically with eB.

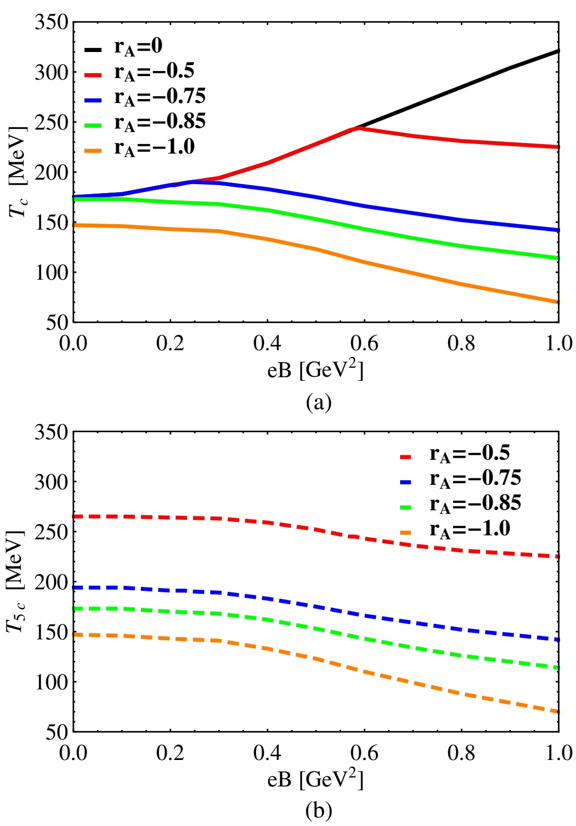

FIG. 3 (color online). T_c and T_{5c} as a function of eB for $r_A = 0$, -0.5, -0.75, -0.85, and -1.0. (a) T_c as a function of eB for different values of r_A. (b) T_{5c} as a function of eB for different values of r_A.

V. CONCLUSIONS

In conclusion, based on the scenario of polarized instanton–anti-instanton molecule pairing above chiral restoration, we provide a dynamical model with a nontrivial repulsive four-quark interaction in the isoscalar axial-vector channel. We observe one unusual property that, in the chirally symmetric phase, there is a first order phase transition for the spontaneous generation of local $\mathcal{P}$ and $\mathcal{CP}$ violation and chirality imbalance. Similar conclusions have been drawn from the studies in the last years, like the discussion in the chiral magnetic effect in heavy ion collisions [64], the NJL model at $\theta = \pi$ [65,66], and the hot linear sigma model with the θ parameter [67,68]. Comparing with previous discussions mentioned above, we propose an effective and straightforward mechanism regarding the local $\mathcal{CP}$ violation by using an unconventional repulsive axial-vector interaction in the NJL model.

In the study of the previous studies, the chirality was always introduced artificially by a finite axial chemical potential as a background physical quantity. Indeed once the axial chemical potential is introduced, the nonzero chirality imbalance is induced and thus it gives a signal to $\mathcal{P}$ and $\mathcal{CP}$ violation in the QCD vacuum, as well as the inverse magnetic catalysis effect. However, it did not give an answer to the mechanism of how the nonzero axial chemical potential is generated from the QCD vacuum without the number difference between right- and left-hand quarks and why it is favored at high temperatures around T_c.

However, in our work, starting from the instanton–anti-intanton molecule model valid for $T \gtrsim T_c$ with nontrivial topological configuration, which is described by the rearrangement of instantons and anti-intantons, an unusual repulsive axial-vector interaction with $G_A < 0$ was found to be produced in the framework of the NJL model [44]. As a consequence, a dynamical chiral chemical potential $\tilde{\mu}_5$, which describes the chirality imbalance, is naturally induced by the axial-vector interaction. And it is obtained that nonzero $\tilde{\mu}_5$, as a vacuum expectation value in the local domains, is preferred over the nonzero chiral condensate σ in the equilibrium of QCD vacuum at high temperatures when $G_A < 0$, which is guaranteed at the temperatures near and above T_c by IIMM. The values of $\tilde{\mu}_5$ could be either positive or negative, depending on the sign of the topological charges in the local domains, but the average value in the whole QCD vacuum should be zero. Moreover, we find that not only the negative sign of G_A is important for the chirality at high temperatures, but also the magnitude of the negative G_A is important for the critical temperature T_{5c}.

Furthermore, when an external magnetic field is added to the QCD vacuum at zero and finite temperatures, we investigate the effects of the magnetic field on the chiral condensate σ and the dynamical chiral chemical potential $\tilde{\mu}_5$. It is found that external magnetic field is the catalyzer of the local chiral imbalance, which destroys the pairing quarks between different chiralities. A reasonable strength of the repulsive interaction in the isoscalar axial-vector channel can naturally explain the inverse magnetic catalysis around critical temperature under external magnetic fields.

With a constant repulsive interaction in the isoscalar axial-vector channel, it is found that the spontaneous generation of the chirality imbalance is of first order phase transition, and when the magnitude of coupling in axial-vector channel is big enough, the chiral phase transition will be locked with the local $\mathcal{CP}$ violation phase transition and will also become a first order phase transition, which is not in agreement with lattice results at finite temperature. This might be improved by considering a temperature dependent coupling constant in the isoscalar axial-vector channel, or considering the spatial structure of the topological charge distribution.

It is worth mentioning that, in Refs. [69] and [70], the local $\mathcal{CP}$ violation effect is also observed in lattice QCD. It is always confusing how local $\mathcal{CP}$ violation can exist in an equilibrium system; the spatial structure of the topological density distribution [71] is helpful to understand this scenario.

As a future project it is straightforward to extend our analysis to the 2+1 flavors and investigate effects of the axial-vector interaction on the chirality imbalance at finite chemical potentials. The chiral magnetic effect is expected to be the natural consequence of quark-gluon plasma in the presence of the strong magnetic field, since local $\mathcal{CP}$ violation and chirality imbalance in the chirally symmetric phase is guaranteed by our mechanism. Besides, we expect this mechanism can have direct application in cosmology related to $\mathcal{CP}$ violation and baryogenesis.

ACKNOWLEDGMENTS

We thank J. Y.Chao, M. Chernodub, T. Kalaydzhyan, and D. N. Li for valuable discussions. This work is supported by the NSFC under Grants No. 11275213 and No. 11261130311 (Grant No. CRC 110 by DFG and NSFC), CAS key project Grant No. KJCX2-EW-N01, and Youth Innovation Promotion Association of CAS. L. Yu is partially supported by China Postdoctoral Science Foundation under Grant No. 2014M550841.

[1] V. Skokov, A. Y. Illarionov, and V. Toneev, Int. J. Mod. Phys. A **24**, 5925 (2009).
[2] V. Voronyuk, V. D. Toneev, W. Cassing, E. L. Bratkovskaya, V. P. Konchakovski, and S. A. Voloshin, Phys. Rev. C **83**, 054911 (2011).
[3] A. Bzdak and V. Skokov, Phys. Lett. B **710**, 171 (2012).
[4] W.-T. Deng and X.-G. Huang, Phys. Rev. C **85**, 044907 (2012).
[5] S. P. Klevansky and R. H. Lemmer, Phys. Rev. D **39**, 3478 (1989).
[6] K. G. Klimenko, Teor. Mat. Fiz. **89**, 211 (1991) [Theor. Math. Phys. **89**, 1161 (1991)].
[7] V. P. Gusynin, V. A. Miransky, and I. A. Shovkovy, Nucl. Phys. **B462**, 249 (1996).
[8] I. A. Shovkovy, Lect. Notes Phys. **871**, 13 (2013).
[9] I. A. Shushpanov and A. V. Smilga, Phys. Lett. B **402**, 351 (1997).
[10] N. O. Agasian and I. A. Shushpanov, Phys. Lett. B **472**, 143 (2000).
[11] J. Alexandre, K. Farakos, and G. Koutsoumbas, Phys. Rev. D **63**, 065015 (2001).
[12] N. O. Agasian, Yad. Fiz. **64**, 608 (2001) [Phys. At. Nucl. **64**, 554 (2001)].
[13] T. D. Cohen, D. A. McGady, and E. S. Werbos, Phys. Rev. C **76**, 055201 (2007).
[14] R. Gatto and M. Ruggieri, Phys. Rev. D **82**, 054027 (2010).
[15] R. Gatto and M. Ruggieri, Phys. Rev. D **83**, 034016 (2011).
[16] A. J. Mizher, M. N. Chernodub, and E. S. Fraga, Phys. Rev. D **82**, 105016 (2010).
[17] K. Kashiwa, Phys. Rev. D **83**, 117901 (2011).
[18] S. S. Avancini, D. P. Menezes, M. B. Pinto, and C. Providencia, Phys. Rev. D **85**, 091901 (2012).
[19] J. O. Andersen, Phys. Rev. D **86**, 025020 (2012).
[20] D. D. Scherer and H. Gies, Phys. Rev. B **85**, 195417 (2012).
[21] P. V. Buividovich, M. N. Chernodub, E. V. Luschevskaya, and M. I. Polikarpov, Phys. Lett. B **682**, 484 (2010).
[22] V. V. Braguta, P. V. Buividovich, T. Kalaydzhyan, S. V. Kuznetsov, and M. I. Polikarpov, Phys. At. Nucl. **75**, 488 (2012).
[23] M. D'Elia, S. Mukherjee, and F. Sanfilippo, Phys. Rev. D **82**, 051501 (2010).
[24] M. D'Elia and F. Negro, Phys. Rev. D **83**, 114028 (2011).
[25] E.-M. Ilgenfritz, M. Kalinowski, M. Muller-Preussker, B. Petersson, and A. Schreiber, Phys. Rev. D **85**, 114504 (2012).
[26] N. O. Agasian and S. M. Fedorov, Phys. Lett. B **663**, 445 (2008).
[27] E. S. Fraga and A. J. Mizher, Nucl. Phys. **A820**, 103c (2009).
[28] E. S. Fraga and L. F. Palhares, Phys. Rev. D **86**, 016008 (2012).
[29] G. S. Bali, F. Bruckmann, G. Endrodi, Z. Fodor, S. D. Katz, S. Krieg, A. Schafer, and K. K. Szabo, J. High Energy Phys. 02 (2012) 044.
[30] G. S. Bali, F. Bruckmann, G. Endrodi, Z. Fodor, S. D. Katz, and A. Schafer, Phys. Rev. D **86**, 071502 (2012).
[31] K. Fukushima and Y. Hidaka, Phys. Rev. Lett. **110**, 031601 (2013).
[32] T. Kojo and N. Su, Phys. Lett. B **720**, 192 (2013).

[33] F. Bruckmann, G. Endrodi, and T. G. Kovacs, J. High Energy Phys. 04 (2013) 112.
[34] J. Chao, P. Chu, and M. Huang, Phys. Rev. D **88**, 054009 (2013).
[35] E. S. Fraga, B. W. Mintz, and J. Schaffner-Bielich, Phys. Lett. B **731**, 154 (2014).
[36] D. E. Kharzeev, L. D. McLerran, and H. J. Warringa, Nucl. Phys. **A803**, 227 (2008).
[37] K. Fukushima, D. E. Kharzeev, and H. J. Warringa, Phys. Rev. D **78**, 074033 (2008).
[38] K. Fukushima, M. Ruggieri, and R. Gatto, Phys. Rev. D **81**, 114031 (2010).
[39] B. I. Abelev *et al.* (STAR Collaboration), Phys. Rev. Lett. **103**, 251601 (2009).
[40] B. I. Abelev *et al.* (STAR Collaboration), Phys. Rev. C **81**, 054908 (2010).
[41] B. Abelev *et al.* (ALICE Collaboration), Phys. Rev. Lett. **110**, 012301 (2013).
[42] E.-M. Ilgenfritz and E. V. Shuryak, Nucl. Phys. **B319**, 511 (1989).
[43] E.-M. Ilgenfritz and E. V. Shuryak, Phys. Lett. B **325**, 263 (1994).
[44] T. Schafer, E. V. Shuryak, and J. J. M. Verbaarschot, Phys. Rev. D **51**, 1267 (1995).
[45] Z. Zhang, Phys. Rev. D **85**, 114028 (2012).
[46] Y. Nambu and G. Jona-Lasinio, Phys. Rev. **122**, 345 (1961).
[47] Y. Nambu and G. Jona-Lasinio, Phys. Rev. **124**, 246 (1961).
[48] S. Klimt, M. F. M. Lutz, U. Vogl, and W. Weise, Nucl. Phys. **A516**, 429 (1990).
[49] U. Vogl and W. Weise, Prog. Part. Nucl. Phys. **27**, 195 (1991).
[50] S. P. Klevansky, Rev. Mod. Phys. **64**, 649 (1992).
[51] T. Hatsuda and T. Kunihiro, Phys. Rep. **247**, 221 (1994).
[52] J. P. Blaizot, E. S. Fraga, and L. F. Palhares, Phys. Lett. B **722**, 167 (2013).
[53] E. V. Shuryak and J. J. M. Verbaarschot, Nucl. Phys. **B410**, 55 (1993).
[54] T. Schafer, E. V. Shuryak, and J. J. M. Verbaarschot, Nucl. Phys. **B412**, 143 (1994).
[55] T. Schafer and E. V. Shuryak, Phys. Rev. D **50**, 478 (1994).
[56] G. 't Hooft, Phys. Rev. D **14**, 3432 (1976); **18**, 2199 (1978).
[57] R. T. Cahill and C. D. Roberts, Phys. Rev. D **32**, 2419 (1985).
[58] P. C. Tandy, Prog. Part. Nucl. Phys. **39**, 117 (1997).
[59] Z. Zhang and W.-Q. Zhao, Phys. Lett. B **610**, 235 (2005).
[60] Z. Zhang and W.-q. Zhao, Phys. Lett. B **612**, 207 (2005).
[61] J. Ashman *et al.* (European Muon Collaboration), Phys. Lett. B **206**, 364 (1988).
[62] M. Buballa, Phys. Rep. **407**, 205 (2005).
[63] T. Schafer and E. V. Shuryak, Rev. Mod. Phys. **70**, 323 (1998).
[64] H. J. Warringa, J. Phys. G **35**, 104012 (2008).
[65] J. K. Boomsma and D. Boer, Nucl. Phys. **A820**, 251C (2009); J. K. Boomsma and D. Boer, *Proc. Sci.*, CONFINEMENT8 (2008) 134 [arXiv:0812.3077].
[66] J. K. Boomsma and D. Boer, Phys. Rev. D **80**, 034019 (2009).
[67] A. J. Mizher and E. S. Fraga, Nucl. Phys. **A831**, 91 (2009).
[68] E. S. Fraga and A. J. Mizher, *Proc. Sci.*, CPOD2009 (2009) 037 [arXiv:0910.4525].
[69] P. V. Buividovich, M. N. Chernodub, E. V. Luschevskaya, and M. I. Polikarpov, Phys. Rev. D **80**, 054503 (2009).
[70] G. S. Bali, F. Bruckmann, G. Endrdi, Z. Fodor, S. D. Katz, and A. Schfer, J. High Energy Phys. 04 (2014) 129.
[71] P. V. Buividovich, T. Kalaydzhyan, and M. I. Polikarpov, Phys. Rev. D **86**, 074511 (2012).